Population dynamics in a metastable neon magneto-optical trap

R. D. Glover,[1] J. E. Calvert,[1,2] and R. T. Sang[1,2,*]

[1]*Centre for Quantum Dynamics, Griffith University, Nathan, Queensland 4111, Australia*

[2]*ARC Centre of Excellence for Coherent X-Ray Science, Griffith University, Nathan, Queensland 4111, Australia*

(Received 9 December 2012; published 20 February 2013)

We observe the population dynamics within a metastable neon magneto-optical trap (MOT) through the measurement of the average squared Clebsch-Gordan coefficient C^2 over a range of laser detunings. The magnitude of C^2 is dependent on the internal quantum state of an atom interacting with the light field and is found to show a strong dependence on the applied laser detuning. Previously it has been reported [Townsend *et al.*, Phys. Rev. A **52**, 1423 (1995)] that trapped atoms in a MOT are pumped towards the states that interact most strongly with the local field and therefore the measured value of C^2 is larger than the average over all possible transitions. For the $^3P_2$-to-$^3D_3$ cooling transition in metastable neon the average C^2 value is equal to 0.46; however, we have measured $0.29 \pm 0.03 < C^2 < 0.73 \pm 0.09$. We explain this range of values for C^2 by considering the possible transition rates between the different magnetic sublevels in the system. This result has significant consequences when trap populations are measured via fluorescence in a MOT.

DOI: 10.1103/PhysRevA.87.023415 PACS number(s): 32.80.Xx

I. INTRODUCTION

The magneto-optical trap (MOT) has become a standard experimental tool in atomic physics. For many experiments involving atomic samples produced in a MOT, it is important to have an accurate knowledge of the fraction of atoms in the excited state. A common method for estimating the atom number and density is based on accurately measuring the fluorescence and excited-state fraction (ESF) in the MOT [1–7]. In addition, an accurate knowledge of atomic populations is crucial for cold collision experiments where different species can have vastly different collisional parameters [8–11]. The ESF is also an important parameter for studies investigating decay dynamics and lifetimes in MOTs [12].

The fractional population of the excited state in a MOT is related to the scattering rate ξ for an atom in an optical field and is given by $\Pi_e = \xi/\Gamma$, where Γ is the linewidth of the atomic transition in rad s^{-1}. In the simple case of a two-level atom in an optical field, the standard textbook definition for the scattering rate is [13]

$$\xi = \frac{\Gamma}{2}\left[\frac{\Omega^2/2}{\delta^2 + \Gamma^2/4 + \Omega^2/2}\right], \tag{1}$$

where δ is the detuning of the incident light field in rad s^{-1} and Ω is the Rabi frequency, given by

$$\Omega = \frac{-E_0}{\hbar}\langle 2|e\hat{r}\cdot\hat{\epsilon}|1\rangle. \tag{2}$$

Here e is the elementary charge of an electron, E_0 is the amplitude of the electric field, $\hat{r}$ is the electron coordinate with respect to the atom's center of mass, $\hat{\epsilon}$ is a unit vector in the direction of polarization of the electric field, and $\langle 1|$ and $|2\rangle$ represent the initial and final states of the single-photon dipole-allowed transition. The matrix element $\langle 2|e\hat{r}\cdot\hat{\epsilon}|1\rangle$ defines the coupling between the dipole moment of the atom $\hat{\mu} = e\hat{r}$ and the incident light field.

Equation (1) is commonly used to estimate the ESF given the trapping-laser detuning and intensity. In reality, the geometry of a MOT leads to a much more complicated system. The energy of the internal atomic state and the electric field polarization are position dependent, and generally the scattering rate is a function of all the possible transitions between the various Zeeman sublevels for the ground and excited states. Various models have been developed to account for the atomic multilevel nature in the MOT [14–16]; however the most commonly used was first proposed by Townsend *et al.* [16] in a cesium MOT. In this work the authors account for this complexity by modifying Eq. (1) for the scattering rate as

$$\xi = \frac{\Gamma}{2}\left[\frac{C_1^2\Omega^2/2}{\delta^2 + \Gamma^2/4 + C_2^2\Omega^2/2}\right], \tag{3}$$

where C_1^2 and C_2^2 are average squared Clebsch-Gordan coefficients. It was expected that C_1^2 and C_2^2 would be of equal magnitude and close to the value of 0.4 found by averaging over all the possible transitions and polarizations in Cs. However, Townsend *et al.* reported that it was insufficient to take the values for C_1^2 and C_2^2 as the average for all transitions and polarizations. Both average squared Clebsch-Gordan coefficients were measured to be approximately equal, $C_1^2 \simeq C_2^2 = 0.7 \pm 0.2$, and significantly larger than the expected value of 0.4. The interpretation was that, in general, the radiation field optically pumps the atom towards the Zeeman substate that interacts most strongly with the local field, resulting in an increased scattering rate.

Equation (3) is commonly used to determine excited-state populations in MOTs [5–12,17]. However, due to the complications involved in accurately measuring a value for the average squared Clebsch-Gordan coefficient, it has been common to adopt a value of $C^2 = 0.7 \pm 0.2$ for all atomic species. The validity of using Eq. (3) to calculate the ESF was demonstrated by Shah *et al.* [18] in a rubidium MOT using a *model-independent* charge-transfer technique. However, the validity of adopting $C^2 = 0.7 \pm 0.2$ as being independent

*r.sang@griffith.edu.au

of the parameter space under investigation has not been sufficiently explored.

In addition to an accurate measurement of the excited-state population, the measurement of C^2 allows information regarding the average internal quantum state of atoms in the MOT to be inferred. Since the value of C^2 primarily depends on the m_j state of the atom interacting with the light field, it is possible to investigate MOT population dynamics by adjusting experimental parameters such as the frequency detuning of the trapping laser.

We extend previous measurements by investigating the the value of C^2 in a metastable neon MOT over a range of laser detunings. It is found that the measured value of C^2 varies widely over the detuning range investigated, indicating significant changes in the population dynamics of the MOT. At large frequency detunings we measure the value of $C^2 = 0.73 \pm 0.09$, which is consistent with the work of Townsend *et al.* [16]. In addition, these results use Ne as the species of interest, and a range of detunings is identified where the approximation of a particular value for C^2 is valid.

II. TECHNIQUE

The technique we use to measure the average squared Clebsch-Gordan coefficient is developed on a saturated-fluorescence method established by DePue *et al.* [19]. The method is based on measuring the fluorescence when the cooling transition is saturated where the ESF is $\frac{1}{2}$. This is achieved through frequency-tuning the MOT laser beams to the atomic resonance and ramping up the intensity, thereby saturating the transition. In this high-intensity limit, the scattering rate can be inferred from the resulting fluorescence signal and is simply $\xi = N\Gamma/2$, where N is the total atom number. The technique was originally used for accurately measuring the phase-space density in a MOT and has since been established as a convenient method for determining atom number [20–22]. The advantage of this method is that it depends on very few assumptions and only the efficiency of the imaging system is required to measure the atomic population.

The technique can be extended to measure the excited-state population in a MOT [21]. In this scheme, two measurements of the fluorescence are made: The first is made at the desired trapping intensity I and detuning δ for which the ESF is being determined. The second measurement is a saturated measurement with the detuning set to the atomic resonance and the intensity sufficient for saturation, $I_{\rm sat}$. The ESF is calculated by the ratio $\Pi_e = f/2f_{\rm sat}$, where f and $f_{\rm sat}$ are the measured fluorescence at the trapping intensity and the saturation intensity, respectively. The values of C_1^2 and C_2^2 can be inferred from Eq. (3) if the total intensity of the light incident on the trapped atoms is well characterized. To avoid the inaccuracies associated with measuring Π_e absolutely, we make a number of fluorescence measurements over a large range of intensities and extract the desired parameters by fitting to the resulting data. This method can be used to determine the coefficient C_2^2. A subsequent measurement can be made to determine C_1^2. However, if the common approximation that $C_1^2 \simeq C_2^2 = C^2$ is made, then only a single measurement is required. By performing the measurement using this fitting method there is no need to make absolute measurements of the atom number or excited-state fraction, and hence uncertainties as a result of absolute calibrations are removed.

It is expected that C_1^2 and C_2^2 are approximately equal in magnitude, and in this work we also make the approximation $C_1^2 \simeq C_2^2$. There are a number of instances in the literature where an equivalent approximation is made; for example, as part of their investigation Shah *et al.* [18] conclude that a one-parameter model is sufficient for modeling the excited-state fraction in a MOT. Alternative methods for modeling the excited-state fraction [14,15] incorporate a single scaling factor that is attached to the saturation intensity to account for the complexities of the MOT. In [15] the saturation intensity which appears in both the numerator and denominator of the appropriate equation is left as a floating variable during the analysis. This method is equivalent to making the assumption that the two average squared Clebsch-Gordan coefficients in Eq. (3) are equal. In [14] a more complex three-parameter model is developed, where two parameters are effective Clebsch-Gordan coefficients. However, in this model the two Clebsch-Gordan coefficients account for the low- and high-intensity regimes and the third parameter describes the crossover point between the two regimes.

Experimentally it is convenient to measure the intensity and frequency detuning of the MOT laser beams. Therefore Ω is expressed in terms of the on-resonance saturation parameter

$$s_0 = \frac{2|\Omega|^2}{\Gamma^2} = \frac{I}{I_0}, \tag{4}$$

where $I = \frac{1}{2}(\epsilon_0 c E_0^2)$ is the laser intensity and I_0 is the saturation intensity, given by

$$I_0 = \frac{\pi hc}{3\lambda^3 \tau}. \tag{5}$$

Here, λ and $\tau = 1/\Gamma$ are the wavelength and natural lifetime of the atomic transition, respectively. By substituting Eq. (4) into Eq. (3) the scattering rate can be reexpressed and it follows that the ESF is

$$\Pi_e = \frac{1}{2}\left[\frac{C^2 s_0}{1 + C^2 s_0 + 4\delta^2/\Gamma^2}\right]. \tag{6}$$

Here the approximation has been made that $C_1^2 \simeq C_2^2 = C^2$. We measure C^2 from Eq. (6) by keeping the detuning δ constant and measuring the fluorescence counts, proportional to Π_e, as a function of the laser intensity $0 < I < I_{\rm sat}$.

The apparatus used in this investigation has been described in detail elsewhere [9,10]. Essentially it consists of a MOT for trapping metastable neon in the $^3P_2$ state that is loaded from a Zeeman-slowed atomic beam. Metastable neon has a conveniently located closed optical transition between the $^3P_2$ and the $^3D_3$ states ($\lambda = 640.2$ nm) which we use for laser cooling. The light for the slowing beam passes through the trapping region and modifies the trapping potential; however, the detuning is typically 8Γ and has a negligible effect on the trapped atoms. A Coherent 899 single-mode, ring dye laser operated using Kiton red laser dye is used to produce the MOT laser beams. The locking scheme utilizes saturated-fluorescence spectroscopy on an isolated sample of metastable neon atoms [23]. The detuning of the laser frequency is controlled by placing a dc magnetic field across the isolated atomic sample which Zeeman-shifts the atomic resonance.

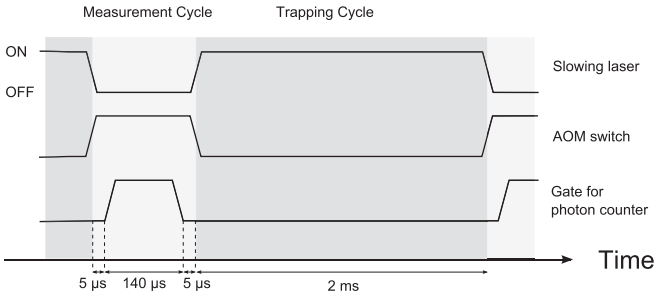

FIG. 1. The timing scheme of the measurement. The measurement cycle lasts a total of 150 μs with a duty cycle of 500 Hz.

Typically the total laser intensity (found by summing the contributions from each of the six trapping laser beams) is $I = 15I_0$ and the magnetic field gradient across the MOT is operated at 13.5 G cm^{-1}. For these parameters approximately 10^6 atoms are trapped.

To ensure that the number of atoms in the MOT remains constant during the measurement, the laser intensity is modulated on a time scale that does not perturb the atom cloud. The period during which the laser intensity is modulated is referred to as the measurement cycle and lasts 150 μs. A duration of 150 μs is chosen based on experimental constraints and is found to be sufficient for acquiring a favorable signal-to-noise ratio while maintaining a regular atom population. During the measurement cycle, the light for the Zeeman slower is switched off, the MOT light intensity is modulated using an acousto-optic modulator (AOM) (IntraAction model, AOM-40), and the fluorescence is measured using an integrated photon counter (Ames Photonics model, Oculus 8010). A 5 μs delay before and after activation of the integrated photon counter ensures that the signal is due only to fluorescence produced during the measurement cycle; see Fig. 1. For a duty cycle of 500 Hz we find that the disturbance to the trap is minimal and there are no cumulative effects due to successive measurements that result in a significant change to the number of atoms in the MOT.

To characterize the total intensity of light incident on the trapped atoms, both the intensity profile of the MOT laser beams and the spatial overlap with the atom cloud are required. The MOT laser beams are made relatively large compared to the atom cloud such that the intensity is relatively uniform across the trap. To measure the spatial profile of the atom cloud, the $\frac{1}{e^2}$ diameter is found by observing the fluorescence on a CCD camera and fitting a Gaussian. For $\delta = 2\Gamma$ and $I = 15I_0$ the trap $\frac{1}{e^2}$ diameter is measured to be 920 ± 10 μm.

The width of the MOT laser beams is found by performing a knife edge measurement. The light for the MOT is transported from the Coherent 899 dye laser to the apparatus via a single-mode optical fiber. The subsequent output coupler and lens system results in a collimated beam with an approximately Gaussian profile. The $\frac{1}{e^2}$ diameter of the beam is found by fitting to the standard definition of the error function,

$$P_x = \frac{P_{\text{tot}}}{2}\left[1 + \text{erf}\left(\frac{x - x_0}{(w/2)}\right)\right], \tag{7}$$

where P_x is the power measured at the position x, P_{tot} is the total power in the beam, x_0 is the center of the beam, and w is the $\frac{1}{e^2}$ diameter of the beam. The knife edge measurement is made at a distance of 2.5 m from the fiber output to simulate the path taken to the MOT region and results in a $\frac{1}{e^2}$ diameter of 8.85 ± 0.06 mm. The intensity in each of the trapping beams is measured and equalized using a power meter that has been calibrated in accordance with the NIST standard (ISO 10012-1).

Since the MOT laser beams are relatively large compared to the atom cloud, the spatial overlap of each of the trapping beams with the atoms in the MOT must be measured. Special care is taken to ensure that the trap is central by initially aperturing the MOT laser beams and optimizing the system. This ensures that the overlap of the two Gaussians is central and allows the contribution from each beam to be considered equivalent. The incident intensity due to a single laser beam can then be found by integrating over the $\frac{1}{e^2}$ diameter of the atom cloud. Therefore the value of s_0 is simply found by summing the total effect due to all six trapping beams, where a scaling factor is introduced for the retroreflected beams to account for these beams making multiple passes through the viewports on the trapping chamber.

III. RESULTS

To make a measurement of the average squared Clebsch-Gordan coefficient, the measured fluorescence from the integrated photon counter is plotted as a function of the incident light intensity. A background signal is first recorded and subsequently subtracted from the measured fluorescence signal. Figure 2 shows a measurement of C^2 for a laser detuning of $\delta = 1.5\Gamma$. The measurement of the fluorescence is un-normalized and therefore a two-parameter fit is made using Eq. (6). The first fitting parameter corresponds to a value of C^2 equal to 0.35 ± 0.04. The second fitting parameter corresponds to the saturated fluorescence and is related to the ESF. Since we are interested only in the value of C^2 from the fit, we do not directly measure the ESF, and at the point where the fluorescence counts are saturating it cannot be assumed that

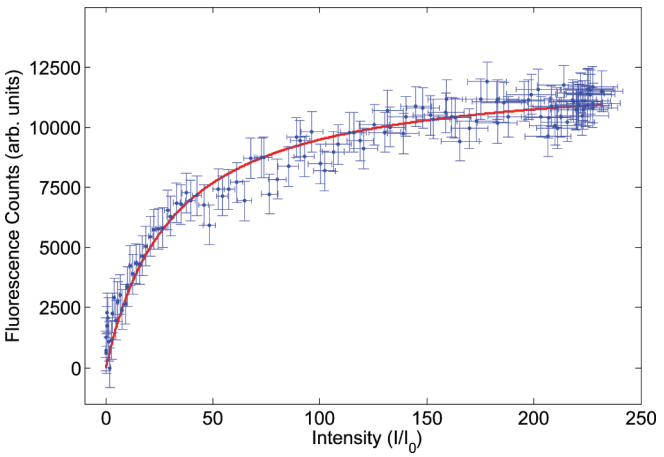

FIG. 2. (Color online) A graph showing the fluorescence from the Oculus photodiode as a function of the incident light intensity. The detuning is $\delta = 1.5\Gamma$ and the fit using Eq. (6) gives $C^2 = 0.35 \pm 0.04$. The ESF is not directly measured; instead an additional fitting parameter is introduced to account for the un-normalized fluorescence counts.

the ESF is equal to 50% since the laser is not resonant with the atomic transition.

The error bars in Fig. 2 are due to counting statistics and are the uncertainty in the fluorescence counts due to processes that are represented by a Poissonian distribution. Laser intensity fluctuations are uncorrelated in time and are included in these statistics. Systematic uncertainties originate from measurement of the laser beam intensity and detuning. As a result of the Gaussian laser beam, the intensity over the trapping potential is nonuniform. The magnitude of the intensity at the $\frac{1}{e^2}$ radius of the trap is approximately 91.5% of the intensity in the center of the trap. The intensity that we use to calculate the C^2 coefficient is an averaged intensity and therefore we include a systematic uncertainty of $\pm 5\%$. This value is overestimated since the majority of the atoms will be located close to the center of the trap where the intensity profile is flatter. The frequency detuning of the laser has a small uncertainty due to the stability of the frequency reference. The long-term locking occurs via an error signal derived through the modulation of a saturated absorption spectrum in a gas discharge cell. The uncertainty introduced as a result of this method is estimated to be at most 10% of the applied detuning. In addition, the MOT quadrupole field shifts the detuning as a function of position in the trap. We estimate the uncertainty at the edge of the trapped atom cloud as a result of the quadrupole field to be less than 0.1Γ. The uncertainty in the measured value of C^2 is found by taking the statistical uncertainty calculated as a part of the fitting routine to one standard deviation, and adding it in quadrature with the uncertainty in the laser intensity. The uncertainty in the frequency detuning of the laser is included in Fig. 3.

Because the measured value of C^2 is dependent on the quantum state of the atom, the population statistics between the available atomic states can be inferred. The variance in C^2 as the detuning of the MOT laser beams is modified is an indication of the changing population dynamics of the trapped atoms. Figure 3 shows the variation in C^2 ($0.29 \pm 0.03 < C^2 < 0.73 \pm 0.09$) as the laser detuning is scanned in the range $1\Gamma < \delta < 4\Gamma$. These results demonstrate the detuning dependence of the light-atom coupling in a MOT, which is due to optical pumping between fine-structure atomic states.

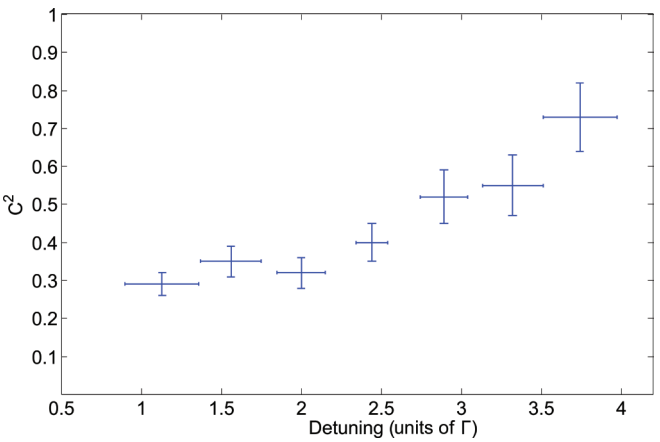

FIG. 3. (Color online) The average squared Clebsch-Gordan coefficient as a function of the laser detuning.

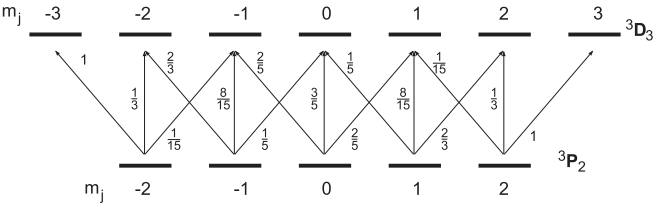

FIG. 4. The squared Clebsch-Gordan coefficient for all the possible $J = 2 \rightarrow J = 3$ fine-structure transitions.

A value of 4Γ represents an upper limit to the detuning and is dependent on experimental constraints. Below 1Γ the trap is observed to become unstable.

The calculated squared Clebsch-Gordan coefficients C^2_{ge} for all the possible $J = 2 \rightarrow J = 3$ fine structure transitions are shown in Fig. 4. The subscripts g and e represent the ground and excited m_j states and identify the fine-structure transition. Since the magnitude of Ω for any particular transition depends on the Clebsch-Gordan coefficients, it follows that the strength of the coupling between the atom and the light field is also dependent on the Clebsch-Gordan coefficients. Generally, the atom will be pumped towards the state that couples most strongly with the local field. For σ^+ light the atom is pumped more efficiently into the $m_j = 2$ to $m_j = 3$ transition, and for σ^- light the atom is pumped towards the $m_j = -2$ to $m_j = -3$ transition. At large detunings the atoms couple more strongly with only one laser beam and hence are optically pumped to the larger-m_j states. Here C^2 approaches an upper limit and measurements at large detunings are consistent with the previous results, where $C^2 = 0.7 \pm 0.2$ [16].

In the case of smaller detunings the measured C^2 is observed to drop towards a value of $C^2 = 0.29 \pm 0.03$. Here it appears that the atom is pumped by both the incident and retroreflected beams and tends towards the $m_j = 0$ state where the calculated squared Clebsch-Gordan coefficient is <1. For atoms in the $m_j = 0$ state the description is more complicated as many more transitions are possible. In addition the resonance condition for σ^+ and σ^- light varies across the trap and will modify the probability of any specific transition occurring. For example, the probability of driving an atom that is in the $m_j = 1$ state with a σ^- photon increases. The squared Clebsch-Gordan coefficient for this transition is relatively small, $C^2_{10} = 0.2$, and as a result, the measured value of $C^2 = 0.29 \pm 0.03$ is lower than the value of 0.46 obtained by averaging over all possible transitions. Therefore the commonly used interpretation that the C^2 value tends to be larger than the average is insufficient, especially in traps where small detunings are used. Inspection of Fig. 3 shows a clear regime change that occurs at approximately 2Γ where the atom switches from being pumped towards the $m_j = 0$ state and begins to be more efficiently pumped into states with higher m_j numbers.

IV. CONCLUSION

We have shown that the population dynamics within a MOT changes dramatically with laser detuning and this has significant effects on the measured average squared Clebsch-Gordan coefficients. We explain the range of the C^2

coefficients using a simple optical-pumping model where the strength of the coupling between the atom and light field in the MOT is related to the Rabi frequency, given in Eq. (2). The results show that on average the most heavily populated m_j state in the MOT is a function of the applied detuning. The technique we have described here can be used as a template for investigating the value of C^2 in other atomic species over a range of laser detunings.

Our measurements over the detuning range $1\Gamma < \delta < 4\Gamma$ in a metastable neon MOT show that the value of C^2 can vary by approximately a factor of 3. This result is significant for measurements of the ESF in a MOT and highlights the importance of making a saturated measurement [19–22] when estimating the ESF. However, sometimes it is convenient to estimate the ESF given only the intensity and detuning of the light incident on the trap; in this case, it is necessary to determine the value C^2 for the range of experimental parameters under investigation.

ACKNOWLEDGMENTS

This research was supported by the Australian Research Council (DP Grant No. DP0208713) and Griffith University. J.E.C. was supported by the Australian Research Council.

[1] F. Bardou, O. Emile, J. M. Courty, C. I. Westbrook, and A. Aspect, Europhys. Lett. **20**, 681 (1992).
[2] J. J. McClelland and J. L. Hanssen, Phys. Rev. Lett. **96**, 143005 (2006).
[3] F. Y. Loo, A. Brusch, S. Sauge, M. Allegrini, E. Arimondo, N. Andersen, and J. Thomsen, J. Opt. B: Quantum Semiclassical Opt. **6**, 81 (2004).
[4] X. Xu, T. H. Loftus, J. L. Hall, A. Gallagher, and J. Ye, J. Opt. Soc. Am. B **20**, 968 (2003).
[5] A. Browaeys, J. Poupard, A. Robert, S. Nowak, W. Rooijakkers, E. Arimondo, L. Marcassa, D. Boiron, C. Westbrook, and A. Aspect, Eur. Phys. J. D **8**, 199 (2000).
[6] Y. Miroshnychenko, A. Gaëtan, C. Evellin, P. Grangier, D. Comparat, P. Pillet, T. Wilk, and A. Browaeys, Phys. Rev. A **82**, 013405 (2010).
[7] C. Gabbanini, A. Evangelista, S. Gozzini, A. Lucchesini, A. Fioretti, J. H. Müller, M. Colla, and E. Arimondo, Europhys. Lett. **37**, 251 (1997).
[8] S. J. M. Kuppens, J. G. C. Tempelaars, V. P. Mogendorff, B. J. Claessens, H. C. W. Beijerinck, and E. J. D. Vredenbregt, Phys. Rev. A **65**, 023410 (2002).
[9] K. J. Matherson, R. D. Glover, D. E. Laban, and R. T. Sang, Rev. Sci. Instrum. **78**, 073102 (2007).
[10] K. J. Matherson, R. D. Glover, D. E. Laban, and R. T. Sang, Phys. Rev. A **78**, 042712 (2008).
[11] R. D. Glover, J. E. Calvert, D. E. Laban, and R. T. Sang, J. Phys. B **44**, 245202 (2011).
[12] M. Zinner, P. Spoden, T. Kraemer, G. Birkl, and W. Ertmer, Phys. Rev. A **67**, 010501 (2003).
[13] H. J. Metcalf and P. van der Straten, *Laser Cooling and Trapping* (Springer, New York, 1999).
[14] J. Javanainen, J. Opt. Soc. Am. B **10**, 572 (1993).
[15] T. P. Dinneen, C. D. Wallace, K.-Y. N. Tan, and P. L. Gould, Opt. Lett. **17**, 1706 (1992).
[16] C. G. Townsend, N. H. Edwards, C. J. Cooper, K. P. Zetie, C. J. Foot, A. M. Steane, P. Szriftgiser, H. Perrin, and J. Dalibard, Phys. Rev. A **52**, 1423 (1995).
[17] B. J. Claessens, J. P. Ashmore, R. T. Sang, W. R. MacGillivray, H. C. W. Beijerinck, and E. J. D. Vredenbregt, Phys. Rev. A **73**, 012706 (2006).
[18] M. H. Shah, H. A. Camp, M. L. Trachy, G. Veshapidze, M. A. Gearba, and B. D. DePaola, Phys. Rev. A **75**, 053418 (2007).
[19] M. T. DePue, S. L. Winoto, D. J. Han, and D. S. Weiss, Opt. Commun. **180**, 73 (2000).
[20] R. G. Dall and A. G. Truscott, Opt. Commun. **270**, 255 (2007).
[21] R. G. Dall, K. G. H. Baldwin, L. J. Byron, and A. G. Truscott, Phys. Rev. Lett. **100**, 023001 (2008).
[22] S. S. Hodgman, R. G. Dall, L. J. Byron, K. G. H. Baldwin, S. J. Buckman, and A. G. Truscott, Phys. Rev. Lett. **103**, 053002 (2009).
[23] B. T. H. Varcoe, B. V. Hall, G. Johnson, P. M. Johnson, W. R. MacGillivray, and M. C. Standage, Meas. Sci. Technol. **11**, N111 (2000).